

ACBP and cholesterol differentially alter fatty acyl CoA utilization by microsomal ACAT

Hsu Chao,* Minglong Zhou,[†] Avery McIntosh,[†] Friedhelm Schroeder,[†] and Ann B. Kier^{1,*}

Department of Pathobiology,* Texas A&M University, TVMC College Station, TX 77843-4467; and

Department of Physiology and Pharmacology,[†] Texas A&M University, TVMC College Station, TX 77843-4466

Abstract Microsomal acyl CoA:cholesterol acyltransferase (ACAT) is stimulated *in vitro* and/or in intact cells by proteins that bind and transfer both substrates, cholesterol, and fatty acyl CoA. To resolve the role of fatty acyl CoA binding independent of cholesterol binding/transfer, a protein that exclusively binds fatty acyl CoA (acyl CoA binding protein, ACBP) was compared. ACBP contains an endoplasmic reticulum retention motif and significantly colocalized with acyl-CoA cholesteryl acyltransferase 2 (ACAT2) and endoplasmic reticulum markers in L-cell fibroblasts and hepatoma cells, respectively. In the presence of exogenous cholesterol, ACAT was stimulated in the order: ACBP > sterol carrier protein-2 (SCP-2) > liver fatty acid binding protein (L-FABP). Stimulation was in the same order as the relative affinities of the proteins for fatty acyl CoA. In contrast, in the absence of exogenous cholesterol, these proteins inhibited microsomal ACAT, but in the same order: ACBP > SCP-2 > L-FABP. The extracellular protein BSA stimulated microsomal ACAT regardless of the presence or absence of exogenous cholesterol. Thus, ACBP was the most potent intracellular fatty acyl CoA binding protein in differentially modulating the activity of microsomal ACAT to form cholesteryl esters independent of cholesterol binding/transfer ability.—Chao, H., M. Zhou, A. McIntosh, F. Schroeder, and A. B. Kier. ACBP and cholesterol differentially alter fatty acyl CoA utilization by microsomal ACAT. *J. Lipid Res.* 2003. 44: 72–83.

Supplementary key words microsome • acyl CoA cholesterol acyltransferase • acyl CoA binding protein

Acyl-CoA:cholesterol acyltransferase (ACAT) is a key enzyme involved in cellular fatty acid and cholesterol homeostasis (1). By transacylating long chain fatty acyl CoA (LCFA-CoA) to cholesterol, ACAT is responsible for the synthesis of cholesteryl esters, the major storage form of cholesterol in the cell. Two isoforms of ACAT (ACAT1 and ACAT2) have been identified in mammals (1–3). ACAT1 accounts for most ACAT activity present in human

liver, adrenal gland, macrophages, and kidney but not intestines (4). In contrast, ACAT2 represents the majority of ACAT activity in human intestine and fetal liver, and the minority of ACAT activity in hepatocytes (5, 6). Despite these advances, the exact physiological roles of ACAT1 and ACAT2 in different tissues and species remain to be elucidated. Since ACATs are integral membrane proteins residing primarily in rough endoplasmic reticulum of various cell types (7), ACAT activities are enriched in the microsomal fraction (8). Because the microsomal ACAT cholesterol substrate pool is not saturated, most previous studies focused on cholesterol availability as rate limiting in ACAT activity (1). Consequently, relatively little is known regarding the other substrate, LCFA-CoA, the acyl chain specificity of ACAT, or the potential role of LCFA-CoA binding proteins in regulating LCFA-CoA availability to ACAT.

The total cellular concentration of LCFA-CoA is between 5–160 μ M, depending on cell and tissue type (9, 10). However, since LCFA-CoAs readily partition into membranes and/or interact with a variety of intracellular LCFA-CoA binding proteins, the free unbound LCFA-CoA pool is in the low nM range and unlikely to exceed 200 nM (10). Thus, under normal physiological conditions, LCFA-CoAs may actually not be readily available as substrates for microsomal ACAT. While the LCFA-CoA substrate specificity (i.e., acyl chain length and unsaturation) of a purified ACAT has not been reported (11), early studies using rat liver microsomes showed that ACAT exhibits specificity in the order: oleoyl-CoA, palmitoyl-CoA, stearoyl-CoA, and linoleoyl-CoA (12). All of these LCFA-CoAs are bound with high affinity by intracellular lipid binding proteins that interact with both ACAT substrates, LCFA-CoA and cholesterol. The intracellular sterol carrier protein-2 (SCP-2) binds both LCFA-CoAs and cholesterol (13) with

Abbreviations: ACAT1, acyl-CoA cholesteryl acyltransferase 1; ACAT2, acyl-CoA cholesteryl acyltransferase 2; ACBP, acyl-CoA binding protein; LCFA-CoA, long chain fatty acyl-CoA; L-FABP, liver fatty acid binding protein; SCP-2, sterol carrier protein-2.

¹ To whom correspondence should be addressed.

e-mail: akier@cvm.tamu.edu

Manuscript received 8 May 2002 and in revised form 20 September 2002.

Published, JLR Papers in Press, October 1, 2002.

DOI 10.1194/jlr.M200191JLR200

high affinity. Likewise, the intracellular liver fatty acid binding protein (L-FABP) binds both LCFA-CoAs (14) and cholesterol (15), albeit with lower affinities. Although SCP-2 (13) and L-FABP (16) stimulate microsomal ACAT activity in vitro and/or in transfected cells, it is unclear whether their activation of microsomal ACAT is due to binding/transferring LCFA-CoA substrate and/or cholesterol substrate to the ACAT enzyme.

In contrast to LCFA-CoAs, a considerable body of knowledge has accumulated regarding the other microsomal ACAT substrate, i.e., cholesterol. Microsomal ACAT activity is clearly regulated by cholesterol, apparently by two distinct mechanisms: First, cholesterol may serve as an activator of purified ACAT (1). Plots of microsomal ACAT versus cholesterol mole fraction in donor membrane vesicles as well as cholesterol substrate saturation curves for recombinant ACAT in reconstituted membrane vesicles are sigmoidal (1, 17). Second, cholesterol substrate supply appears to be rate-limiting under physiological conditions (1). Very little of the endogenous microsomal cholesterol is available as a substrate for ACAT and, thus, cholesterol must be transferred to the microsomal ACAT from exogenous sources (1). Because of cholesterol's very low aqueous solubility, spontaneous transfer of exogenous cholesterol (i.e., from other membranes such as plasma membrane) is normally very slow (18, 19), but is dramatically enhanced in the presence of the intracellular lipid binding protein sterol carrier protein-2 both in vitro and in transfected cells expressing SCP-2 (18–20). The ability of SCP-2 to stimulate microsomal ACAT was originally attributed to SCP-2 binding and transferring cholesterol to microsomal ACAT for esterification (20). However, as indicated above, the observation that sterol carrier protein-2 binds LCFA-CoAs with high affinity (i.e., nM K_d s) (21) obscures this interpretation. SCP-2 alters the domain structure of cholesterol in potential cholesterol donor membranes (e.g., plasma membrane, lysosomes, and mitochondria) and acceptor membranes (i.e., endoplasmic reticulum) both in vitro and in transfected cells (18). Thus, SCP-2 may thereby increase the availability of exogenous cholesterol and facilitate entry of exogenous cholesterol to microsomal ACAT by altering the membrane domain structure of cholesterol and accessibility to ACAT therein.

In contrast to SCP-2 and L-FABP, which both interact with each ACAT substrates (i.e., cholesterol and LCFA-CoAs) (13), acyl CoA binding protein (ACBP) has high affinity and exclusively binds only LCFA-CoAs (9). The purpose of the studies presented herein was 4-fold: *i*) to examine the interrelationships between LCFA-CoA substrate level and cholesterol substrate availability in contributing to microsomal ACAT activity; *ii*) to utilize ACBP to resolve the potential role of LCFA-CoA binding, independent of cholesterol binding, on the ability of intracellular lipid binding proteins to modulate microsomal ACAT activity; *iii*) to compare the relative effects of LCFA-CoA binding protein versus LCFA-CoA/cholesterol binding proteins on microsomal ACAT activity in the presence and absence of exogenous cholesterol; *iv*) to determine if ACBP is present in endoplasmic reticulum, the intracellular site wherein ACAT is localized.

MATERIALS AND METHODS

Materials

Cholesterol (3 β -hydroxyl-5-cholesten-3-one), triacylglycerol, cholesteryl-oleate, and 1-palmitoyl-2-oleoyl-*sn*-glycerol-3-phosphocholine (POPC) were purchased from Avanti Polar-Lipids (Alabaster, AL). [1 - 14 C]oleoyl CoA (56.3 and 57 mCi/mmol) was obtained from New England Nuclear. Fatty acid free BSA and EDTA were purchased from Sigma (St. Louis, MO). Nitrocellulose membrane was purchased from Schleicher & Schuell (Keene, NH), Sigma, and Bio Rad (Hercules, CA). Sephacryl S-300 beads were acquired from Pharmacia (Uppsala, Sweden). Silica gel G thin-layer chromatography plates were obtained from Analtech (Newark, DE). All other chemicals were reagent grade or better.

Primary antibodies for immunocytochemistry were prepared or obtained as follows: recombinant mouse ACBP was obtained as described in the following section and rat polyclonal anti-ACBP antibodies were prepared against the mouse ACBP as described earlier (22). Polyclonal antisera to ACBP were prepared in rats (Hazleton Research Products, Denver, PA) according to the protocols for the use of laboratory animals approved by the appropriate institutional review committee and met AAALAC guidelines as described earlier (22). Rabbit anti-human acyl-CoA cholesteryl acyltransferase 1 (ACAT1) and rabbit anti-human acyl-CoA cholesteryl acyltransferase 2 (ACAT2) affinity purified IgG (50 μ g/100 μ l PBS containing 0.02% sodium azide) were generously provided by Dr. T. Y. Chang (Department of Biochemistry, Dartmouth Medical School, Hanover, NH). Mouse anti-rough endoplasmic reticulum (clone RF6), which recognizes a 43 kDa antigen in rough ER, was obtained from DAKO Co. (Carpinteria, CA). Secondary antibodies for immunocytochemistry were purchased from the following sources: Texas Red-conjugated goat anti-rat IgG was from Sigma Chemical Co. FITC-conjugated goat anti-rabbit IgG and FITC-conjugated goat anti-mouse IgG were from Jackson ImmunoResearch Laboratories, Inc. (West Grove, PA).

Protein purification

Mouse recombinant ACBP was prepared by inserting the mouse ACBP cDNA as a fusion protein in pET-32 Xa/LIC plasmid vector (Novagen, Madison, WI), expressing in BL21(DE3) bacteria, purifying the fusion protein with S-protein agarose, and cleaving the fusion protein with Factor Xa followed by Xarrest agarose for 30 min. The fusion peptide was removed with Ni-NTA agarose. The final native ACBP product appeared as a single band on silver stained Tricine gel and by Western blotting (not shown). Human recombinant SCP-2 was isolated and purified as described earlier (21). Rat recombinant L-FABP was expressed and purified as previously described (23). Lipid extraction of the purified recombinant proteins did not detect any significant levels of bound ligand. Likewise, BSA was purchased lipid free from Sigma. Protein concentration was determined by Bradford assay (Sigma).

Isolation of rat liver microsomes

Microsomes, prepared from male Sprague-Dawley rat (200–210 g) livers, were washed by gel filtration with 100 ml column volume of Sephacryl S-300 beads to remove trapped soluble lipid binding proteins as described (24). Western blotting analysis showed no detectable amount of ACBP (24) or SCP-2 (25) and only trace amounts of L-FABP (24).

Preparation of cholesterol donor membranes

Small unilamellar vesicles. Small unilamellar vesicles (SUV) were prepared from 1-palmitoyl-2-oleoyl-phosphatidylcholine (POPC) and cholesterol (molar ratio 65:35), basically as described

earlier (26). Although the method used to prepare SUV yields the same cholesterol/POPC molar ratio as in the starting material, the yield of SUV formed is not 100% efficient. Therefore, it was necessary to determine the final cholesterol concentration in each SUV preparation. Lipids were extracted from 5 μ l of SUV preparation using 200 μ l chloroform-methanol (2:1, v/v). Cholesterol was separated from POPC by TLC using a Silica gel G plate and quantitated as described earlier (26).

Measurement of ACAT activity

Microsomal ACAT activity was measured by formation of cholesteryl- $[^{14}\text{C}]$ oleate as follows: Unless indicated in text, the reactions were performed in 50 mM Tris, pH 7.4, 150 mM NaCl, 1 mM EDTA buffer containing 30 μ g of microsome protein, 35 nmol cholesterol (SUV), 30 μ M $[^{14}\text{C}]$ oleoyl-CoA, and designated amounts of fatty acyl-CoA binding protein in a total volume of 50 μ l. As a positive LCFA-CoA binding protein control, fatty acid free BSA was used in the assay instead of intracellular LCFA-CoA binding protein (ACBP, SCP-2, L-FABP). Reaction mixtures without $[^{14}\text{C}]$ oleoyl-CoA were preincubated at 37°C for 30 min. Reactions were initiated by addition of the 30 μ M $[^{14}\text{C}]$ oleoyl-CoA after preincubation and then further incubated for 30 min in a 37°C shaking water bath. The reaction was terminated by addition of 700 μ l of chloroform-methanol (2:1, v/v) and vortexing. Then 500 μ l 50 mM Tris, pH 7.4 buffer, and 50 μ l of 10% KCl were added to each sample followed by vortexing for 1 min and incubation at -20°C for at least 2 h to extract the lipids. Samples were then centrifuged for 2 min at top speed in a bench top centrifuge. The aqueous layer containing $[^{14}\text{C}]$ oleoyl-CoA was transferred to a scintillation vial and radioisotope was quantified in liquid scintillation cocktail (Scinti Verse, Fisher Scientific, Pittsburgh, PA) on a Packard 1600TR liquid scintillation counter (Meridian, CT). The organic layer containing the cholesterol esters, acylglycerols, fatty acids, cholesterol, and phospholipids was dried under nitrogen. Individual lipid fractions into which $[^{14}\text{C}]$ oleoyl-CoA was incorporated were resolved by extracting lipids, drying lipids under a stream of nitrogen gas, and spotting the lipids (redissolved in 50 μ l of chloroform) along with standards (cholesteryl oleate, dioleoylglycerol, trioleoylglycerol, oleic acid, cholesterol, phosphatidic acid) in separate lanes on an activated silica gel G plate, and lipids were separated using a solvent system containing petroleum ether-diethyl ether-acetic acid (85:20:1, v/v/v). Lipids were visualized with iodine. By comparison with the known standards, the desired bands were removed by scraping and the radioactivity was determined in liquid scintillation cocktail (Scinti Verse, Fisher Scientific, Pittsburgh, PA) using a Packard 1600 TR scintillation counter (Meridian, CT).

Cell culture

Stock cultures of L-cells (L-arpt^{-tk}) were maintained in 10% FBS Higuchi medium (22). Stock cultures of McA-RH7777 hepatoma cells, a gift of Dr. Charles Baum (Dept. of Medicine, Clinical Nutrition Research Unit, Section of Gastroenterology, Univ. of Chicago, Chicago, IL), were maintained as described (27). For indirect immunofluorescence (see below), cells were grown on glass cover slip chambers and prepared as described earlier (28).

Western blotting

Western blotting and/or protein isolation has shown that both L-cells and hepatoma cells have high levels of ACBP: 0.8 μ g ACBP/mg protein for L-cells (9) 1.8 μ g ACBP/mg protein for McA-RH7777 hepatoma cells (not shown). These levels of ACBP are similar to those reported for mouse and rat liver, i.e., 0.6 μ g ACBP/mg protein (9). To determine whether L-cells or hepatoma cells contain ACAT1 and/or ACAT2, Western blotting was performed with the

anti-human ACAT1 and anti-human ACAT2 at 1:1,000 dilution, basically as described earlier (28). Western blots demonstrated that ACAT2 was detectable in L-cells, ACAT1 was only weakly detectable and insufficient for immunofluorescence imaging in L-cells, and both ACAT1 and ACAT2 were very weakly detectable and insufficient for immunofluorescence imaging in hepatoma cells (data not shown). Therefore, double immunolabeling for colocalization of ACBP with ACAT in rough endoplasmic reticulum by laser scanning confocal microscopy was possible only with anti-ACAT2 with L-cells. To colocalize ACBP with rough endoplasmic reticulum in hepatoma cells, another endoplasmic reticulum marker was used, anti-rough endoplasmic reticulum (cloneRF6, recognizing a 43 kDa antigen of rough endoplasmic reticulum).

Double immunolabeling and confocal fluorescence microscopy

Double immunolabeling, laser scanning confocal microscopy (LSCM), and image analysis were performed as described earlier (28). Briefly, L-cells and hepatoma cells were fixed immediately with 1 ml of cold methanol-acetone (1:1, v/v) per well (4-well chamber slide) and incubated at -20°C for 10 min. The fixative solution was then discarded and the cover glass air-dried. The cover glass was then blocked with 2% goat serum-BSA in PBS (pH 7.4) for 1–1.5 h at room temperature (or overnight at 4°C). A 0.2 ml of primary antibodies diluted in blocking solution was added to each well and incubated at room temperature for 1 h. Multiple dilutions of primary and secondary antibodies were tested. Optimal dilutions of primary antibodies were: 1:50 rat anti-mouse ACBP polyclonal antibodies (for detecting ACBP), 1:10 mouse anti-rough endoplasmic reticulum (clone RF6, for detecting rough endoplasmic reticulum), and 1:50 rabbit anti-human ACAT2 (for detecting rough endoplasmic reticulum). The solution containing the primary antibodies was then removed, and the cover slip washed in PBS containing 0.05% Tween-20 for 20–30 min (five times). The secondary antibody, diluted in blocking buffer or PBS, was then added to the cover slip and incubated for 1 h at room temperature. The optimal dilution for all secondary antibodies was 1:100: Texas Red-conjugated goat anti-rat IgG antibody, FITC-conjugated goat anti-rabbit IgG antibody, and FITC-conjugated goat anti-mouse IgG antibody. The secondary antibody solution was then removed followed by five washes of the cover slip with PBS over a 20–30 min time period. The cells were then imaged by laser scanning confocal microscopy as previously described (28). FITC was visualized by Kr/Ar laser excitation at 488 nm and detecting fluorescence emission through a 522/DF35 filter (Chroma Technology Corp., Brattleboro, VT). Texas red was excited by the 568 nm Kr/Ar laser line and fluorescence detected through a HQ598/40 emission filter (Chroma Technology Corp., Brattleboro, VT). As controls for all immunolocalization studies, cells were incubated with primary or secondary antibody alone.

Statistical analysis

Values represent the mean \pm SE. Statistical significance was evaluated with Student's *t*-test.

RESULTS

Microsomal acyl-CoA:cholesterol transferase

Effect of increasing oleoyl CoA in the absence of exogenous cholesterol. In the absence of exogenous oleoyl CoA and exogenous cholesterol donor (i.e., SUV cholesterol), microsomal ACAT activity (measured as transacylation of $[^{14}\text{C}]$ oleoyl-CoA

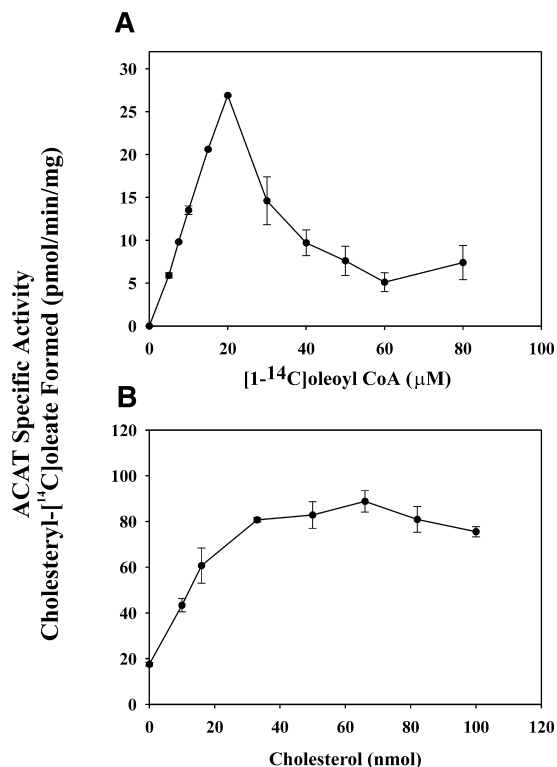


Fig. 1. Effect of oleoyl CoA on microsomal ACAT. A: Effect of oleoyl-CoA on ACAT specific activity in the absence of exogenous cholesterol. Reactions containing 5 micrograms microsome protein were preincubated at 37°C for 30 min, then initiated by adding [1-¹⁴C]oleoyl-CoA and incubated for another 4 min at 37°C. B: Effect of exogenous cholesterol on ACAT activity. Five μg microsome protein and various amount of cholesterol were preincubated for 30 min at 37°C, initiated by adding 40 μM [1-¹⁴C]oleoyl-CoA and incubated for 5 min at 37°C. Reactions were stopped by adding 700 μl of chloroform-methanol (2:1, v/v) and vortexing. Lipid extraction, TLC, and counting the cholesteryl-[1-¹⁴C]oleate bands were performed as described in Materials and Methods.

with cholesterol to form cholesteryl-[1-¹⁴C]oleate) was essentially non-detectable (Fig. 1A, 0 μM oleoyl CoA). To determine if endogenous microsomal cholesterol was available for esterification by ACAT, increasing amount of substrate oleoyl-CoA over a broad range (0 μM, 5 μM, 7.5 μM, 10 μM, 15 μM, 20 μM, 30 μM, 40 μM, 50 μM, 60 μM, and 80 μM) was added in the absence of exogenous cholesterol. Microsomal ACAT activity increased to a maximum of 26.8 pmol/min/mg protein at 20 μM oleoyl CoA (Fig. 1A). Oleoyl CoA concentrations >20 μM inhibited the microsomal ACAT by 82% (4.8 pmol/min/mg protein) at 60 μM oleoyl (Fig. 1A).

Thus, even in the absence of exogenous cholesterol, a small pool of cholesterol is available for microsomal ACAT to be stimulated. In the absence of exogenous cholesterol, such a low level of microsomal ACAT activity has been attributed to spontaneous redistribution of cholesterol among microsomal fragments (17). The fact that at >20 μM oleoyl CoA the microsomal ACAT was inhibited may be due in part to the detergent-like properties of high levels of fatty acyl CoAs (29). Similar inhibition of other types of microsomal acyltransferases (e.g., glycerol-

3-phosphate acyltransferase) has also been reported, albeit at much higher oleoyl CoA concentrations, i.e., >80 μM (30). These data suggest that in the absence of exogenous cholesterol donor, the microsomal ACAT is 4-fold more sensitive to inhibition by oleoyl CoA than other microsomal acyltransferases.

Effect of increasing exogenous cholesterol on microsomal ACAT. To test the effect of exogenous cholesterol on microsomal ACAT, cholesterol was added to the assay in the form of small unilamellar vesicles (SUV) composed of 1-palmitoyl-2-oleoyl-phosphatidylcholine (POPC) and cholesterol (65:35 molar ratio). These model membranes were used to deliver exogenous cholesterol because cholesterol has very poor aqueous solubility and cholesterol-rich membranes are the normal substrate source of intracellular cholesterol for microsomal ACAT. The cholesterol/POPC ratio used herein was similar to that typical for cell surface membranes.

With increasing exogenous cholesterol and constant oleoyl CoA, microsomal ACAT activity increased in linear fashion to 60.7 pmol/min/mg protein at 20 μM cholesterol (Fig. 1B). At cholesterol concentrations >33 μM, microsomal ACAT activity plateaued near 80.4 pmol/min/mg protein (Fig. 1B). Microsomal ACAT activity in the presence of exogenous cholesterol reached a plateau that was 3-fold higher than observed that in the absence of cholesterol (Fig. 1A) and 8.5-fold more that determined at the same concentration of oleoyl CoA (40 μM oleoyl CoA) but without exogenous cholesterol (Fig. 1A). Thus, exogenous cholesterol enhanced microsomal ACAT to a much higher level than the small pool of endogenous microsomal cholesterol available to microsomal ACAT by spontaneous transfer of cholesterol between microsomal fragments.

To determine if microsomal ACAT activity was maximal in the presence of the above concentration of exogenous cholesterol donor, the quantity of microsomal protein was increased from 5 μg to 120 μg. Total cholesteryl-[1-¹⁴C]oleate (pmol/min) formed by microsomal ACAT increased linearly up to 120 μg microsomal protein (Fig. 2A), indicating that the exogenous cholesterol donor was still in sufficient excess for testing the effects of added fatty acyl CoA binding proteins. Finally, increasing the incubation time to longer than 30 min did not further increase the amount of cholesteryl-[1-¹⁴C]oleate (Fig. 2B).

Microsomal acyl-CoA:cholesterol transferase

Effect of increasing oleoyl CoA in the presence of exogenous cholesterol. Since high levels of oleoyl CoA inhibited microsomal ACAT in the absence of exogenous cholesterol, it was important to determine if addition of exogenous cholesterol prevented this effect. In the presence of exogenous cholesterol, microsomal ACAT activity increased linearly from 0 μM to 60 μM oleoyl CoA and reached maximal values at 60–80 μM oleoyl CoA (Fig. 2C). The maximum was 36.6-fold higher than that obtained with equivalent oleoyl-CoA for microsomal ACAT activity without exogenous cholesterol (Fig. 1A). Furthermore, at high concentrations of oleoyl CoA (e.g., 100 μM) microsomal ACAT activity was inhibited only slightly, 4%, in the presence of exogenous cholesterol (Fig. 2C). Thus, with exogenous cholesterol,

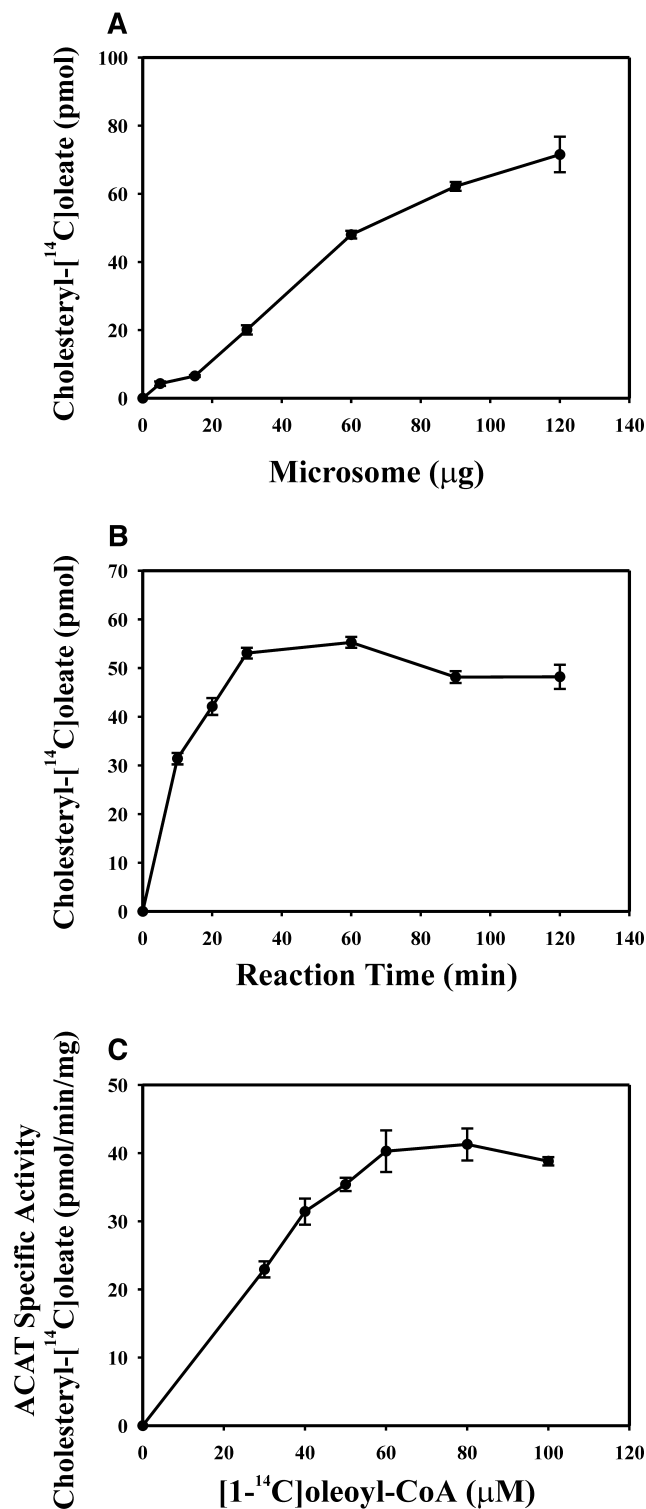


Fig. 2. Optimization of microsomal ACAT A: Optimization of amount of microsomal protein for the ACAT assays. Reactions containing 72 nmol of cholesterol and a designated amount of microsomal protein (0–120 μg) were preincubated at 37°C for 30 min, initiated by adding 40 μM [^{14}C]oleoyl-CoA and incubated for another 30 min. B: Reaction time optimization. Mixtures containing 60 μg of microsomal protein and 72 nmol of cholesterol were preincubated at 37°C for 30 min, initiated by adding 30 μM [^{14}C]oleoyl-CoA and incubated for designated times at 37°C. C: Effect of oleoyl-CoA on ACAT activity with exogenous cholesterol. Reactions contained 30 μg microsomal protein and 72 nmol cholesterol were preincubated at 37°C for 30 min, initiated by adding 30 μM [^{14}C]oleoyl-CoA and incubated for another 20 min. Seven hundred microliters of chloroform-methanol (2:1, v/v) were added to stop reaction and lipid extraction, TLC, and counting cholesteryl-[^{14}C]oleate were performed as described in Materials and Methods.

the inhibitory effect of high oleoyl CoA was 21-fold smaller (i.e., 4% vs. 82% inhibition), and shifted to 5-fold higher oleoyl CoA concentration.

Comparison of the time course of microsomal ACAT in the absence versus presence of exogenous cholesterol revealed additional differences. While both curves were linear during the first 5 min, in the absence of cholesterol, microsomal ACAT activity reached maximal value by 10 min (Fig. 3). In contrast, with exogenous cholesterol, mi-

croosomal ACAT continued to increase, albeit 2-fold more slowly, such that even by 45 min the activity had not plateaued.

In summary, ACAT activity was regulated not only by availability of both substrates, but in the presence of exogenous cholesterol the inhibitory effect of high levels of oleoyl CoA was essentially abolished. Only in the presence of exogenous cholesterol did microsomal ACAT activity respond optimally to the increased oleoyl-CoA availability.

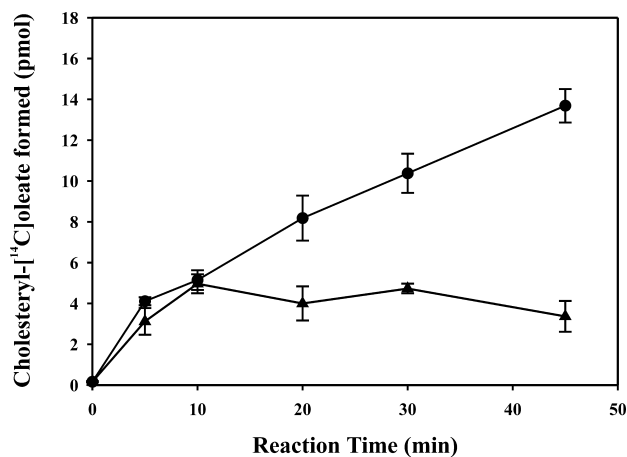


Fig. 3. Effect of exogenous cholesterol on optimized microsomal ACAT. Reactions containing 80 nmol exogenous cholesterol (circles) or no exogenous cholesterol (triangles) were mixed with 30 μ g microsomal protein, warmed at 37°C for 2 min, and initiated by adding 30 μ M [1-¹⁴C]oleoyl-CoA. Mixtures were then incubated for designated times at 37°C and terminated by adding 700 μ l of chloroform-methanol (2:1, v/v). Lipid extraction, TLC, and counting cholesteryl-[1-¹⁴C]oleate were performed as described in Materials and Methods.

These findings suggested that the choice of assay conditions, which resulted in marked differences in ACAT activity, could determine at least in part the effect of LCFA-CoA binding proteins on microsomal ACAT activity.

Intracellular fatty acyl CoA binding proteins (ACBP, SCP-2, and L-FABP) inhibit ACAT in the absence of exogenous cholesterol

Since activity of microsomal ACAT measured in the absence of exogenous cholesterol donor, was inhibited at >20 μ M oleoyl CoA (Fig. 1A), the possibility that addition of LCFA-CoA binding proteins may remove the inhibitory effect was examined using three intracellular fatty acid binding proteins with a wide range of affinity for fatty ACBP with \leq 2 nM K_d (31); sterol carrier protein-2 (SCP-2) with 3–5 nM K_d (21); liver fatty acid binding protein (L-FABP) with 2–3 orders of magnitude lower affinity, i.e., K_d s in the submicromolar to micromolar range (14).

In the absence of exogenous cholesterol, microsomal ACAT activity was inhibited by all three intracellular LCFA-CoA binding proteins in rank order roughly following their K_d s: ACBP > sterol carrier protein-2 (SCP-2) > liver fatty acid binding protein (L-FABP) (Fig. 4). While at a low level of LCFA-CoA binding protein (i.e., 15 μ M) only ACBP significantly inhibited microsomal ACAT activity (by 30%), at 30 μ M all three proteins significantly ($P < 0.05$) inhibited microsomal ACAT by 48% (ACBP), 16% (SCP-2), and 8% (L-FABP), respectively (Fig. 4). These effects were specific to intracellular LCFA-CoA binding proteins. Addition of an extracellular protein that binds LCFA-CoA binding (e.g., BSA) stimulated microsomal ACAT activity by as much as 46% (Fig. 4). These data suggest that in the absence of exogenous cholesterol, the intracellular, but not extracellular, LCFA-CoA binding proteins inhibited microsomal ACAT. Interestingly, the protein that specifi-

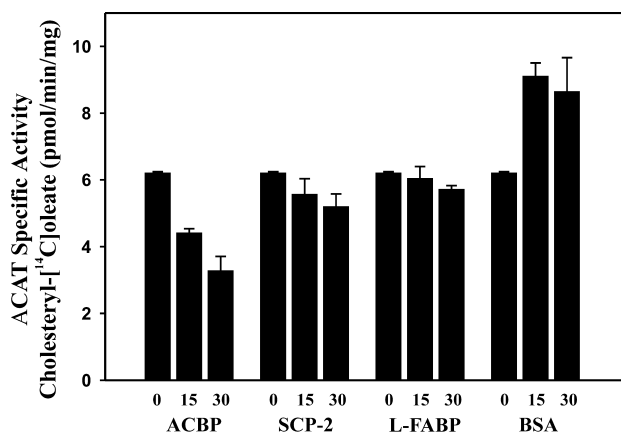


Fig. 4. The inhibitory effects of acyl-CoA binding protein (ACBP), sterol carrier protein-2 (SCP-2), and liver fatty acid binding protein (L-FABP) on microsomal ACAT in the absence of exogenous cholesterol. Reactions containing 30 μ g microsome protein and a designated lipid binding protein (0, 15, and 30 μ M) were warmed 2 min at 37°C before initiating reactions by adding 30 μ M [1-¹⁴C]oleoyl-CoA. Mixtures were incubated at 37°C for 30 min and stopped by adding 700 μ l chloroform-methanol (2:1, v/v) and vortexing. Lipid extraction, TLC, and counting cholesteryl-[1-¹⁴C]oleate were performed as described in Materials and Methods.

cally binds only LCFA-CoAs, i.e., ACBP, exhibited the greatest inhibitory effect on microsomal ACAT.

Role of exogenous cholesterol in determining the effect of intracellular fatty acyl CoA binding protein on microsomal ACAT

In the presence of exogenous cholesterol, addition of all the intracellular fatty acyl CoA binding proteins stimulated microsomal ACAT by as much as 2.6-fold, depending on the specific LCFA-CoA binding protein (Fig. 5). At low levels of intracellular LCFA-CoA binding proteins (i.e., 10 μ M) the stimulation followed in the order: ACBP (2.6-fold) > SCP-2 (1.4-fold), L-FABP (1.5-fold) (Fig. 5). However, at higher level of LCFA-CoA binding protein (i.e., 30 μ M) ACBP and SCP-2 exhibited nearly equivalent stimulation, 2.4-fold and 2.2-fold respectively. L-FABP did not increase further than the 1.5-fold stimulation already noted at lower concentration. This stimulatory effect of LCFA-CoA binding proteins on microsomal ACAT was not specific to intracellular LCFA-CoA binding proteins. Addition of an extracellular protein that also binds LCFA-CoA (i.e., BSA) also stimulated microsomal ACAT activity by 1.6-fold and 1.9-fold at 10 μ M and 30 μ M BSA, respectively (Fig. 5).

In summary, these data show for the first time that the intracellular LCFA-CoA binding proteins (ACBP, SCP-2, L-FABP) differentially stimulated microsomal ACAT depending on the amount of exogenous cholesterol. While all three proteins inhibited microsomal ACAT in the absence of exogenous cholesterol, in contrast all three proteins stimulated microsomal ACAT in the presence of exogenous cholesterol. These differential effects of the intracellular LCFA-CoA binding proteins on microsomal ACAT were specific, since the extracellular LCFA-CoA binding protein BSA

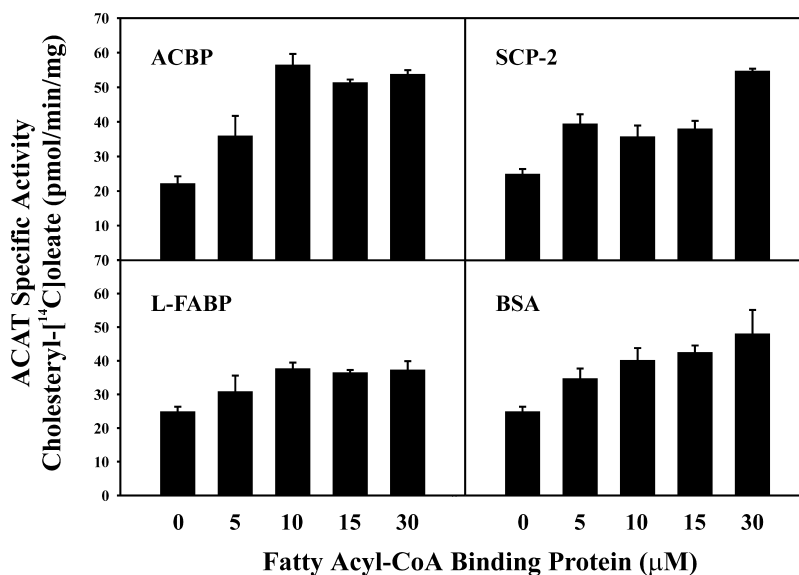


Fig. 5. Effect of fatty acyl CoA binding proteins on microsomal ACAT in the presence of exogenous cholesterol. Reactions containing 30 µg microsome protein and designated concentrations of lipid binding protein (0 µM, 5 µM, 10 µM, 15 µM, and 30 µM) were preincubated at 37°C for 30 min and initiated by adding 30 µM [1-¹⁴C]oleoyl-CoA. Mixtures were incubated for 30 min at 37°C and stopped by adding 700 µl of chloroform-methanol (2:1, v/v). Lipid extraction, TLC, and counting cholesteryl-[1-¹⁴C]oleate were performed as described in Materials and Methods.

stimulated microsomal ACAT regardless of the absence or presence of exogenous cholesterol.

Stimulation of microsomal ACAT by fatty acyl CoA binding protein

Effect of fatty acyl CoA substrate form. The effect of LCFA-CoA substrate form was examined by initiating the microsomal ACAT assay in the presence of exogenous cholesterol under the following conditions (**Table 1**): Control: preincubating for 30 min with no binding protein, followed by initiation of ACAT reaction by adding oleoyl CoA; Condition A: preincubating for 30 min with LCFA-CoA binding protein, followed by initiation of ACAT reaction by adding oleoyl CoA; Condition B, preincubating for 30 min without a LCFA-CoA binding protein or oleoyl CoA, followed by initiation of reaction by addition of a LCFA-CoA binding protein:oleoyl CoA complex. The latter was performed by incubation of LCFA-CoA binding protein with oleoyl CoA for 10 min at room temperature. The effects of Conditions A and B were normalized to the Control.

As expected, all three intracellular LCFA-CoA binding proteins stimulated microsomal ACAT when the reaction was initiated by addition of oleoyl CoA substrate (Table 1, Condition A). However, addition of the oleoyl CoA as a LCFA-CoA binding protein:oleoyl CoA complex was a significantly more effective than adding oleoyl CoA alone for initiating the microsomal ACAT reaction (Table 1, Condition B): ACBP, 2.9-fold versus 1.6-fold; SCP-2, 2.7-fold versus 2.3-fold; and L-FABP, 2.8-fold versus 2.1-fold. The latter enhancement of microsomal ACAT was not observed when the LCFA-CoA binding protein:oleoyl CoA complex formation was preincubated in the presence of 5% etha-

nol (data not shown), since ethanol disrupts ligand interactions with lipid binding proteins (32). These results indicated that the binding of LCFA-CoA ligand to binding protein is important in stimulating ACAT activity.

Intracellular colocalization of ACBP with ACAT2 in the endoplasmic reticulum of L-cell fibroblasts

In order for the preceding observations showing that intracellular LCFA-CoA binding proteins enhance ACAT in the endoplasmic reticulum to be functionally significant, it was important to determine if these proteins localize in the endoplasmic reticulum. Although SCP-2 and L-FABP are localized in highest concentration in peroxisomes and cytoplasm, respectively, low amounts of SCP-2 (13) and L-FABP

TABLE 1. Effect of fatty acyl-CoA form on ACAT activity

Initiation of ACAT Assay	ACBP	SCP-2	L-FABP
Unbound oleoyl-CoA	1.60 ± 0.55	2.34 ± 0.19 ^a	2.00 ± 0.08 ^a
Protein bound oleoyl-CoA	2.92 ± 0.04 ^a	2.59 ± 0.01 ^a	2.84 ± 0.30 ^a

Reactions containing 30 µg microsome protein but no lipid binding protein were initiated by adding 30 µM [1-¹⁴C]oleoyl-CoA. Mixtures containing 30 µM microsome protein and 30 µM lipid binding protein were preincubated at 37°C for 10 min and initiated by adding 30 µM [1-¹⁴C]oleoyl-CoA. Reactions with 30 µM microsome protein were preincubated at 37°C for 10 min and initiated by adding 30 µM lipid binding protein/30 µM [1-¹⁴C]oleoyl-CoA complex. The oleoyl-CoA/lipid binding protein complex was made by incubating 30 µM [1-¹⁴C]oleoyl-CoA with 30 µM lipid binding protein at RT for 10 min. Mixtures were incubated at 37°C for 10 min and stopped by adding 700 µl of chloroform-methanol (2:1, v/v) and vortexing. Lipid extraction, TLC, and counting the cholesteryl-[1-¹⁴C]oleate were performed as described in Materials and Methods.

^a $P < 0.005$ ($n = 6$).

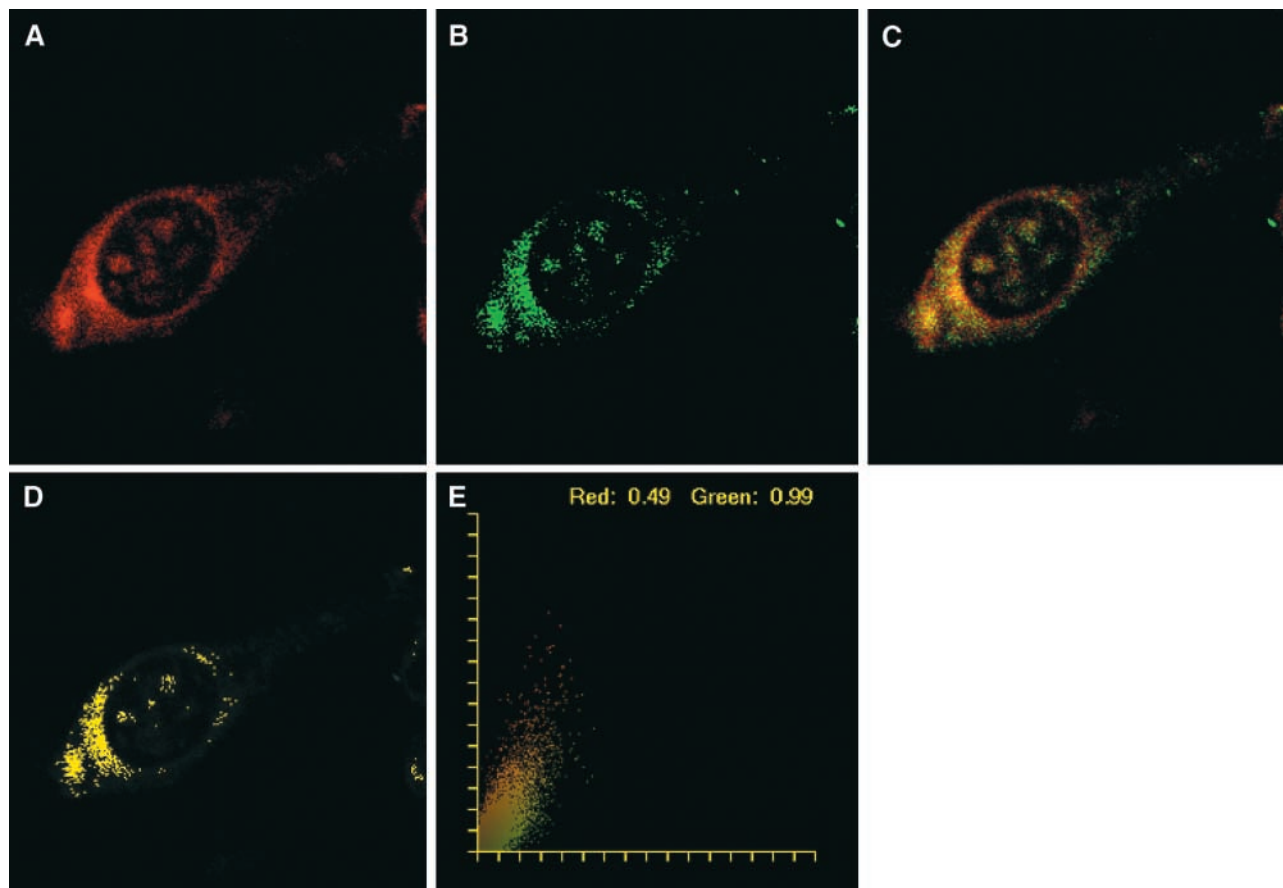


Fig. 6. Colocalization of ACBP with acyl-CoA cholesteryl acyltransferase 2 (ACAT2) in endoplasmic reticulum of L-cell fibroblasts. Double immunolabeling with (A) Texas Red-conjugated goat anti-rat IgG to detect ACBP (red) and (B) FITC-conjugated goat anti-rabbit IgG to detect ACAT2, followed by simultaneous acquisition of laser scanning confocal microscopic images was performed as described in Materials and Methods. C: Simultaneously acquired images A and B were superimposed to yield a merged image. ACBP colocalized with ACAT2 appeared as yellow-orange pixels. D: Image showing only the ACBP that colocalized with ACAT2. Pixel fluorogram of the merged image showing the higher degree of ACBP and ACAT2 fluorescence spatial correlation: red:green 0.49, green:red 0.99.

(33) are also present in the endoplasmic reticulum. In contrast, almost nothing is known regarding the intracellular localization of ACBP, much less whether it is localized to any extent in endoplasmic reticulum. L-cell fibroblasts contain high levels of ACBP (9), exhibit ACAT activity (16), and express ACAT2 (see Materials and Methods). Therefore, L-cells were double immunolabeled with antisera to ACBP and ACAT2 to determine if ACBP is present in rough endoplasmic reticulum. ACAT2 is localized in rough endoplasmic reticulum (6, 7).

L-cells double immunolabeled with anti-ACBP and anti-ACAT2 were imaged by laser scanning confocal microscopy (LSCM). A representative 0.3μ confocal slice through the cell and its nucleus (darker area in middle of the slice) is shown in **Fig. 6**. The intracellular distribution pattern of anti-ACBP was most intense in the perinuclear region with lower diffuse staining throughout the cytoplasm (**Fig. 6A**). Interestingly, significant levels of Texas Red-conjugated goat anti-rat ACBP IgG staining were also detected in the nucleus in nonrandom distribution (**Fig. 6A**). The strongest FITC-conjugated goat anti-rabbit ACAT2 IgG (green) labeling pattern in L-cells was also highest in the perinuclear region (**Fig. 6B**). However, labeling with FITC-conjugated

goat anti-rabbit ACAT2 IgG was much less intense and very little was localized in the nuclei (**Fig. 6B**). Superposition of the simultaneously acquired fluorescence patterns for Texas Red-conjugated goat anti-rat ACBP IgG (red) and FITC-conjugated goat anti-rabbit ACAT2 IgG (green) revealed significant colocalization, especially in the perinuclear region (**Fig. 6C**). Much of the immunofluorescence appeared as yellow/orange colocalized pixels rather than separate red and green areas (**Fig. 6C**). This was more clearly demonstrated by showing only the colocalized pixels (**Fig. 6D**). Finally, when these qualitative data were displayed as a pixel fluorogram (**Fig. 6E**), many yellow/orange pixels were localized along the diagonal of the fluorogram, suggesting strong colocalization. Few of the FITC-conjugated goat anti-rabbit ACAT2 IgG pixels (green) were distinct from those of Texas Red-conjugated goat anti-rat ACBP IgG (red). The ratio of green pixels colocalizing with red pixels was 0.99, indicating that 99% of anti-ACAT2 antibody colocalized with anti-ACBP antibody in the endoplasmic reticulum. However, significant levels of ACBP were not present in endoplasmic reticulum, as evidenced by the ratio of red pixels colocalizing with green pixels as being only 0.49.

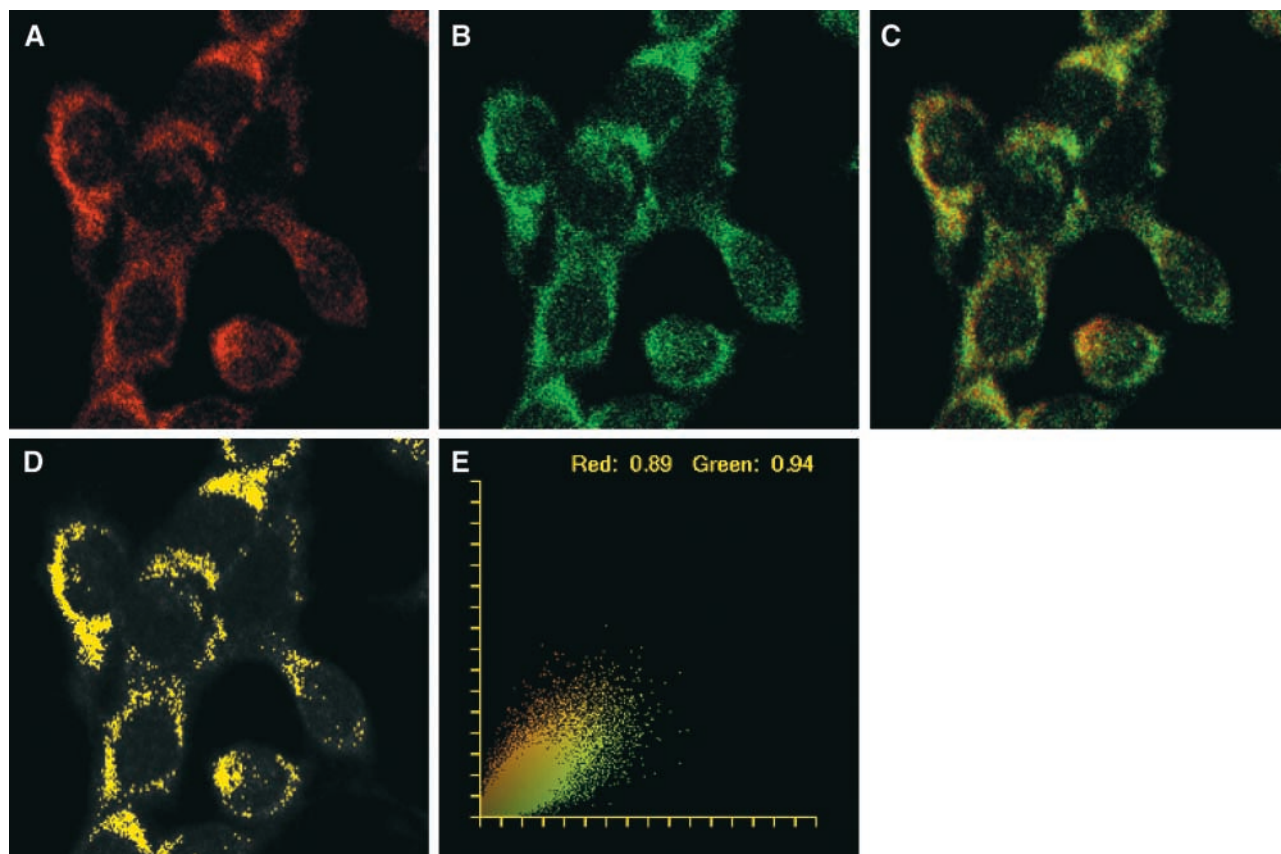


Fig. 7. Colocalization of ACBP with rough endoplasmic reticulum in McA-RH7777 hepatoma cells. Double immunolabeling with (A) Texas Red-conjugated goat anti-rat IgG to detect to detect ACBP (red) and (B) FITC-conjugated goat anti-mouse rough endoplasmic reticulum (clone RF6) marker, followed by simultaneous acquisition of laser scanning confocal microscopic images was performed as described in Materials and Methods. C: Simultaneously acquired images A and B were superimposed to yield a merged image. ACBP colocalized with rough endoplasmic reticulum (clone RF6) marker appeared as yellow-orange pixels. D: Image showing only the ACBP that colocalized ACBP with rough endoplasmic reticulum (clone RF6) marker. Pixel fluorogram of the merged image showing the higher degree of ACBP and rough endoplasmic reticulum (clone RF6) marker fluorescence spatial correlation: red:green 0.89, green:red 0.94.

Colocalization of ACBP with endoplasmic reticulum in hepatoma cells

To determine whether ACBP's colocalization with endoplasmic reticulum ACAT2 in L-cells was a general property, the intracellular localization of ACBP was also examined in McA-RH777 hepatoma cells. Since ACAT1 and ACAT2 were very weakly detectable with the available antibodies in McA-RH777 hepatoma cells, the ACBP was colocalized with another marker for the endoplasmic reticulum: rough endoplasmic reticulum Clone RF6.

McA-RH777 hepatoma cells were fixed and double immunolabeled to detect the ACBP (red) and endoplasmic reticulum (Clone RF6) marker (green), followed by simultaneous colocalization of the two proteins by laser scanning confocal fluorescence microscopy. The McA-RH777 hepatoma cells stained brightly with both Texas Red-conjugated goat anti-rat ACBP IgG (red in **Fig. 7A**) and FITC-conjugated goat anti-mouse rough endoplasmic reticulum (clone RF6) marker IgG pixels (green in **Fig. 7B**). Staining with both antibodies appeared brightest in the perinuclear region, although weaker staining was observed in nuclei of McA-RH777 hepatoma cells. Superposition of the two images (**Fig. 7C**) showed much yellow/

orange labeling as well as some distinct green and red diffuse labeling. This was more clearly evident when only the colocalized pixels were shown (**Fig. 7D**). Again, the highest colocalization was in the perinuclear region along with much weaker staining in the nuclei. This was quantitatively confirmed in the pixel fluorogram (**Fig. 7E**). The pixel fluorogram showed a high population of Texas Red-conjugated goat anti-rat ACBP IgG (red) and FITC-conjugated goat anti-mouse rough endoplasmic reticulum (clone RF6) marker IgG pixels (green) appearing as yellow/orange pixels along the y axis. The ratio of green pixels colocalizing with red pixels was 0.94, indicating that 94% of endoplasmic reticulum marker colocalized with ACBP. However, some ACBP was not present in endoplasmic reticulum as evidenced by the ratio of red pixels colocalizing with green pixels as being slightly less, i.e., 0.89.

DISCUSSION

Cellular cholesterol uptake, storage, and excretion represent an intricate homeostatic balance of cellular cholesterol needs. ACAT is a key enzyme in this regulation since

it catalyzes the microsomal synthesis of cholesteryl esters from fatty acyl CoA and cholesterol. ACAT plays at least three important roles: *i*) ACAT prevents cytotoxicity of excess free cholesterol by converting it into less toxic cholesteryl esters. Because of its poor aqueous solubility, excess free cholesterol crystallizes in tissues (34), cells (35), and membranes (36), where it is cytotoxic. Inhibition of ACAT induces accumulation of unesterified cholesterol and cell toxicity (37). *ii*) ACAT stores excess cholesterol as cholesteryl esters within the cell in cholesteryl ester rich-lipid droplets. Such cholesteryl ester rich-lipid droplets are especially important as sources of cholesterol for corticosteroid production in steroidogenic cells (38). *iii*) ACAT produces cholesterol esters for formation of lipoproteins in liver (VLDL) and intestine (chylomicrons) for transport to other tissues. The results presented herein provide several new insights to potential regulation of ACAT activity in the endoplasmic reticulum by fatty acyl CoA binding protein, independent of cholesterol binding.

First, not only cholesterol but also LCFA-CoA levels potentially regulate the activity of ACAT *in vitro*. Interestingly, microsomal ACAT was inhibited in the presence of physiological levels of LCFA-CoAs (i.e., >20 μ M) (9). The latter observation may account for the low level of ACAT activity under physiological conditions where cholesterol substrate supply is low (17). In contrast, under conditions of high exogenous cholesterol availability, the LCFA-CoA inhibition was removed or shifted to >5-fold higher oleoyl CoA concentration. While the molecular basis for the simple addition of exogenous cholesterol donor resulting in increased ACAT may be attributed to increased availability of cholesterol (12), the increase may equally be due to the high LCFA-CoA binding capacity of membranes (10). The exogenous cholesterol used in the microsomal ACAT assay was added as small unilamellar vesicles (POPC-cholesterol, 65:35, v/v) composed of a single bilayer membrane. Due to their small size (SUV have a limiting radius of curvature near 290 Å), the membrane surface area available to provide LCFA-CoA binding sites is very high (39). By adding SUV as an exogenous cholesterol donor, the inhibitory LCFA-CoA may be removed by reversible binding of excess LCFA-CoA to the SUV membranes, yet still readily available as a microsomal ACAT substrate.

Second, the results for the first time resolved a long-standing issue regarding whether intracellular lipid binding proteins enhanced microsomal ACAT by interaction with fatty acyl CoA, independent of interaction with cholesterol. Although ACBP exclusively binds fatty acyl CoAs (9), ACBP stimulated microsomal ACAT by 3–8-fold, but only in the presence of exogenous cholesterol. This effect was specific for intracellular fatty acyl CoA binding proteins with ACBP > SCP-2 > L-FABP, an order roughly following the relative affinities of these proteins for fatty acyl CoAs. Although BSA also stimulated liver microsomal ACAT, it had no effect on human mononuclear phagocyte microsomal ACAT (40). The reason for the discrepancy is unclear, but may be due to the source of BSA, the lipidation state of the BSA, and/or the fact that the two ACATs may not be the same. Finally, the present data


also confirm an earlier observation (40) that, in the absence of exogenous cholesterol, ACBP inhibits microsomal ACAT.

Third, the data showed for the first time that fatty acyl CoA bound to an intracellular fatty acyl CoA binding protein (e.g., fatty acyl-CoA:ACBP complex) was a better substrate for microsomal ACAT than fatty acyl CoA alone. This finding was supported by the observation that ACBP:fatty acyl CoA complexes donate fatty acyl CoA to microsomal acyltransferases involved in phosphatidic acid biosynthesis (41). Precedent for this potential mechanism comes from parallel studies with microsomal acyl CoA:retinol acyltransferase (ARAT) (42). ARAT functions analogous to ACAT in that ARAT stimulates formation of retinyl-esters, the intracellular storage form of retinol (42). ARAT interacts directly with the holocellular retinol binding protein (containing bound ligand) but not the apocellular retinol binding protein (no bound ligand) (42). The holocellular retinol binding protein may better interact with the microsomal ARAT because the holoretinol binding protein undergoes a conformational change upon ligand binding (43). Likewise, ACBP undergoes a conformational change upon fatty acyl CoA binding (31). ACBP is an ellipsoidal protein (axes of 15 Å and 9 Å) with overall rotational correlation time, based on Trp emission, near 3.1 ns (31). Upon oleoyl CoA binding, rotational correlation time of ACBP decreases by 23% (from 3.1 ns to 2.4 ns, $P < 0.05$), overall hydrodynamic diameter of ACBP decreases by 2 Å, and the segmental motions of Trp residues increase (31). Similar conformational differences in L-FABP isoforms are thought to account for differential modulation of microsomal glycerol-3-phosphate acyltransferase by these isoforms (30).

Fourth, it was shown for the first time that not only ACAT2 (44), but also ACBP were significantly localized in endoplasmic reticulum. Localization of ACBP in endoplasmic reticulum was consistent with the fact that: *i*) the C-terminal amino acid sequence of ACBP (i.e., VDELK KKYGI) contains the endoplasmic retention motif KKKYG (45), and *ii*) ACBP selectively interacts with highly-curved, anionic phospholipid membranes (46). However, since ACBP can readily be solubilized from cell and tissue homogenates, it would appear that ACBP is not a likely transmembrane/integral membrane protein like ACAT1 or ACAT2. Instead, ACBP interacts with membranes primarily through electrostatic forces as has been observed for other fatty acyl CoA binding proteins such as SCP-2 (39) and L-FABP (47). Finally, the observation that ACBP is significantly localized in nuclei of L-cells and hepatoma cells suggests that this protein may be influence nuclear receptors that bind fatty acyl CoAs and thereby regulate the transcriptional activity of genes involved in lipid metabolism as well as glucose uptake (48).

Fifth, *in vitro* exchange assays do not support a mechanism whereby ACBP and other fatty acyl CoA binding proteins stimulate microsomal ACAT by enhancing cholesterol transfer from neutral charged donor SUV to microsomal ACAT. The SUV used herein were comprised of POPC-cholesterol (65:35, v/v), which do not have a net

negative charge. While SCP-2, L-FABP, and BSA all bind cholesterol, such proteins strongly stimulate cholesterol transfer from anionic SUV (e.g., SUV containing negatively charged phospholipids), but not neutral zwitterionic phospholipid containing SUV (49). Fatty acyl CoA/cholesterol binding proteins such as SCP-2 only very weakly enhance sterol transfer from POPC:cholesterol SUV, while L-FABP has no effect (50). ACBP neither binds cholesterol nor enhances sterol transfer in these assays (not shown). Nevertheless, as shown herein, the fatty acyl CoA/cholesterol binding proteins (SCP-2, L-FABP, BSA) stimulate microsomal ACAT in the presence of exogenous cholesterol (POPC:cholesterol SUV) and fatty acyl CoA. Thus, there was little or no correlation between the ability of a fatty acyl CoA/cholesterol binding protein to enhance cholesterol transfer from neutral charged SUV and the ability to stimulate microsomal ACAT in the presence of neutral charged SUV cholesterol donors.

In summary, while the mechanism whereby fatty acyl CoA binding proteins modulate microsomal ACAT activity has not been clearly established, data to date suggest the following possibilities: *i*) since ACBP specifically binds only fatty acyl CoAs and does not directly transfer cholesterol between membranes, ACBP may stimulate microsomal ACAT as the holoprotein (i.e., ACBP containing bound fatty acyl CoA) interacting directly with microsomal ACAT enzyme to provide fatty acyl CoA substrate. *ii*) ACBP may stimulate microsomal ACAT by increasing the aqueous fatty acyl CoA pool. Although membranes have a high capacity to bind fatty acyl CoAs, they do so with low affinity as shown by K_d s near 6 μ M (10). In contrast, ACBP has very high affinity as shown by K_d s of 1–5 nM (9, 31). Thus, ACBP extracts fatty acyl CoAs from membranes (51). *iii*) ACBP may stimulate microsomal ACAT by removing the inhibitory influence of high levels of fatty acyl CoAs. *iv*) ACBP may protect fatty acyl CoAs from microsomal hydrolases and thereby increase the available pool of unhydrolyzed fatty acyl CoA to be used as a substrate by microsomal ACAT. Other fatty acyl CoA binding proteins have been shown to protect fatty acyl CoAs from microsomal hydrolases (23, 52). *v*) ACBP may stimulate microsomal ACAT activity by binding to the microsomal membrane (46), a feature apparently shared with other intracellular fatty acyl CoA binding proteins. 

This work was supported in part by the USPHS and National Institutes of Health Grants GM-31651 and DK-41402.

REFERENCES

1. Chang, T-Y., C. C. Y. Chang, and D. Cheng. 1997. Acyl-coenzyme A:cholesterol acyltransferase. *Annu. Rev. Biochem.* **66**: 613–638.
2. Cases, S., S. Novak, Y. W. Zheng, H. M. Myers, S. R. Lear, E. Sande, C. B. Welch, A. J. Lusis, T. A. Spencer, B. R. Krause, S. K. Erickson, and R. V. Farese. 1998. ACAT-2, a second mammalian acyl CoA cholesterol acyltransferase: its cloning, expression, and characterization. *J. Biol. Chem.* **273**: 26755–26764.
3. Oelkers, P., C. Behl, D. Cromley, J. T. Billheimer, and J. T. Sturley. 1998. Characterization of two human genes encoding acyl coen-

- zyme A: cholesterol acyltransferase-related enzymes. *J. Biol. Chem.* **273**: 26765–26771.
4. Lee, O., C. C. Y. Chang, W. Lee, and T-Y. Chang. 1998. Immunodepletion experiments suggest that acyl-coenzyme A:cholesterol acyltransferase-1 (ACAT-1) protein plays a major catalytic role in adult human liver, adrenal gland, macrophages, and kidney, but not in intestines. *J. Lipid Res.* **39**: 1722–1727.
5. Chang, C. C. Y., N. Sakashita, K. Ornvold, O. Lee, E. T. Chang, R. Dong, S. Lin, C-Y. G. Lee, S. C. Strom, R. Kashyap, J. J. Fung, R. V. Farese, J-F. Patoiseau, A. Delhon, and T. Y. Chang. 2000. Immunological quantitation and localization of ACAT-1 and ACAT-2 in human liver and small intestine. *J. Biol. Chem.* **275**: 28083–28092.
6. Chang, T. Y., C. C. Chang, S. Lin, C. Yu, B. L. Li, and A. Miyazaki. 2001. Roles of acyl CoA:cholesterol acyltransferase-1 and -2. *Curr. Opin. Lipidol.* **12**: 289–296.
7. Sakashita, N., A. Miyazaki, M. Takeya, S. Horiuchi, C. C. Chang, T-Y. Chang, and K. Takahashi. 2000. Localization of human acyl-Coenzyme A:cholesterol acyltransferase-1 (ACAT-1) in macrophages and in various tissues. *Am. J. Path.* **156**: 227–236.
8. Hashimoto, S., and A. M. Fogelman. 1980. Smooth microsomes. A trap for cholesteryl ester formed in hepatic microsomes. *J. Biol. Chem.* **255**: 8678–8684.
9. Gossett, R. E., A. A. Frolov, J. B. Roths, W. D. Behnke, A. B. Kier, and F. Schroeder. 1996. Acyl Co A binding proteins: multiplicity and function. *Lipids.* **31**: 895–918.
10. Knudsen, J., M. V. Jensen, J. K. Hansen, N. J. Faergeman, T. Neergard, and B. Gaigg. 1999. Role of acyl CoA binding protein in acyl CoA transport, metabolism, and cell signaling. *Mol. Cell. Biochem.* **192**: 95–103.
11. Yu, C., J. Chen, S. Lin, J. Liu, C. C. Y. Chang, and T-Y. Chang. 1999. Human acyl-CoA:cholesterol acyltransferase-1 is a homotetrameric enzyme in intact cells and in vitro. *J. Biol. Chem.* **274**: 36139–36145.
12. Billheimer, J. T., and P. J. Gillies. 1990. Intracellular cholesterol esterification. *In Advances in Cholesterol Research.* M. Esfahani and J. B. Swaney, editors. The Telford Press, Caldwell, NJ. 7–45.
13. Gallegos, A. M., B. P. Atshaves, S. M. Storey, O. Starodub, A. D. Petrescu, H. Huang, A. McIntosh, G. Martin, H. Chao, A. B. Kier, and F. Schroeder. 2001. Gene structure, intracellular localization, and functional roles of sterol carrier protein-2. *Prog. Lipid Res.* **40**: 498–563.
14. Frolov, A., T. H. Cho, E. J. Murphy, and F. Schroeder. 1997. Isoforms of rat liver fatty acid binding protein differ in structure and affinity for fatty acids and fatty acyl CoAs. *Biochemistry.* **36**: 6545–6555.
15. Fischer, R. T., M. S. Cowlen, M. E. Dempsey, and F. Schroeder. 1985. Fluorescence of delta 5,7,9(11),22-ergostatetraen-3 beta-ol in micelles, sterol carrier protein complexes, and plasma membranes. *Biochemistry.* **24**: 3322–3331.
16. Jefferson, J. R., J. P. Slotte, G. Nemezc, A. Pastuszyn, T. J. Scallen, and F. Schroeder. 1991. Intracellular sterol distribution in transfected mouse L-cell fibroblasts expressing rat liver fatty acid binding protein. *J. Biol. Chem.* **266**: 5486–5496.
17. Cheng, D., and C. L. Tipton. 1999. Activation of acyl CoA cholesterol acyltransferase: redistribution in microsomal fragments of cholesterol and its facilitated movement by methyl-beta-cyclodextrin. *Lipids.* **34**: 261–268.
18. Schroeder, F., A. M. Gallegos, B. P. Atshaves, S. M. Storey, A. McIntosh, A. D. Petrescu, H. Huang, O. Starodub, H. Chao, H. Yang, A. Frolov, and A. B. Kier. 2001. Recent advances in membrane cholesterol microdomains: rafts, caveolae, and intracellular cholesterol trafficking. *Exp. Biol. Med.* **226**: 873–890.
19. Gallegos, A. M., B. P. Atshaves, S. Storey, A. McIntosh, A. D. Petrescu, and F. Schroeder. 2001. Sterol carrier protein-2 expression alters plasma membrane lipid distribution and cholesterol dynamics. *Biochemistry.* **40**: 6493–6506.
20. Moncecchi, D. M., G. Nemezc, F. Schroeder, and T. J. Scallen. 1991. The participation of sterol carrier protein-2 (SCP-2) in cholesterol metabolism. *In Physiology and Biochemistry of Sterols.* G. W. Patterson and W. D. Nes, editors. American Oil Chemists' Society Press, Champaign, IL. 1–27.
21. Frolov, A., T. H. Cho, J. T. Billheimer, and F. Schroeder. 1996. Sterol carrier protein-2, a new fatty acyl coenzyme A-binding protein. *J. Biol. Chem.* **271**: 31878–31884.
22. Atshaves, B. P., A. Petrescu, O. Starodub, J. Roths, A. B. Kier, and F. Schroeder. 1999. Expression and intracellular processing of the 58 kDa sterol carrier protein 2/3-oxoacyl-CoA thiolase in transfected mouse L-cell fibroblasts. *J. Lipid Res.* **40**: 610–622.
23. Jolly, C. A., D. A. Wilton, and F. Schroeder. 2000. Microsomal fatty acyl CoA transacylation and hydrolysis: fatty acyl CoA species de-

- pendent modulation by liver fatty acyl CoA binding proteins. *Biochim. Biophys. Acta.* **1483**: 185–197.
24. Jolly, C. A., T. Hubbell, W. D. Behnke, and F. Schroeder. 1997. Fatty acid binding protein: stimulation of microsomal phosphatidic acid formation. *Arch. Biochem. Biophys.* **341**: 112–121.
 25. Chao, H., J. T. Billheimer, A. B. Kier, and F. Schroeder. 1999. Microsomal long chain fatty acyl CoA transacylation: differential effect of SCP-2. *Biochim. Biophys. Acta.* **1439**: 371–383.
 26. Huang, H., J. A. Ball, J. T. Billheimer, and F. Schroeder. 1999. The sterol carrier protein-2 amino terminus: a membrane interaction domain. *Biochemistry.* **38**: 13231–13243.
 27. Baum, C. L., E. J. Reschly, A. K. Gayen, M. E. Groh, and K. Schadick. 1997. Sterol carrier protein-2 overexpression enhances sterol cycling and inhibits cholesterol ester synthesis and high density lipoprotein cholesterol secretion. *J. Biol. Chem.* **272**: 6490–6498.
 28. Starodub, O., C. A. Jolly, B. P. Atshaves, J. B. Roths, E. J. Murphy, A. B. Kier, and F. Schroeder. 2000. Sterol carrier protein-2 immunolocalization in endoplasmic reticulum and stimulation of phospholipid formation. *Am. J. Physiol.* **279**: C1259–C1269.
 29. Powell, G. L., P. S. Tippett, T. C. Kiorpes, J. McMillin-Wood, K. E. Coll, H. Schultz, K. Tanaka, E. S. Kang, and E. Shrago. 1985. Fatty acyl CoA as an effector molecule in metabolism. *Fed. Proc.* **44**: 81–84.
 30. Jolly, C. A., E. J. Murphy, and F. Schroeder. 1998. Differential influence of rat liver fatty acid binding protein isoforms on phospholipid fatty acid composition: phosphatidic acid biosynthesis and phospholipid fatty acid remodeling. *Biochim. Biophys. Acta.* **1390**: 258–268.
 31. Frolov, A. A., and F. Schroeder. 1998. Acyl coenzyme A binding protein: conformational sensitivity to long chain fatty acyl-CoA. *J. Biol. Chem.* **273**: 11049–11055.
 32. Schroeder, F., S. C. Myers-Payne, J. T. Billheimer, and W. G. Wood. 1995. Probing the ligand binding sites of fatty acid and sterol carrier proteins: effects of ethanol. *Biochemistry.* **34**: 11919–11927.
 33. Bordewick, U., M. Heese, T. Borchers, H. Robenek, and F. Spener. 1989. Compartmentation of hepatic fatty-acid-binding protein in liver cells and its effect on microsomal phosphatidic acid biosynthesis. *Biol. Chem. Hoppe-Seyler.* **370**: 229–238.
 34. Guo, W., J. D. Morrisett, M. E. DeBakey, G. M. Lawrie, and J. A. Hamilton. 2000. Quantification in situ of crystalline cholesterol and calcium phosphate hydroxyapatite in human atherosclerotic plaques by solid-state magic angle spinning NMR. *Arterioscler. Thromb. Vasc. Biol.* **20**: 1630–1636.
 35. Tangirala, R. K., W. G. Jerome, N. L. Jones, D. M. Small, W. J. Johnson, J. M. Glick, F. H. Mahlberg, and G. H. Rothblat. 1994. Formation of cholesterol monohydrate crystals in macrophage-derived foam cells. *J. Lipid Res.* **35**: 93–104.
 36. Tulenko, T. N., M. Chen, P. E. Mason, and R. P. Mason. 1998. Physical effects of cholesterol on arterial smooth muscle membranes: evidence of immiscible cholesterol domains and alterations in bilayer width during atherogenesis. *J. Lipid Res.* **39**: 947–956.
 37. Warner, G. J., G. Stoudt, M. Bamberger, W. J. Johnson, and G. H. Rothblat. 1995. Cell toxicity induced by inhibition of acyl coenzyme A: cholesterol acyltransferase and accumulation of unesterified cholesterol. *J. Biol. Chem.* **270**: 5772–5778.
 38. Petrescu, A. D., A. M. Gallegos, Y. Okamura, I. J. F. Strauss, and F. Schroeder. 2001. Steroidogenic acute regulatory protein binds cholesterol and modulates mitochondrial membrane sterol domain dynamics. *J. Biol. Chem.* **276**: 36970–36982.
 39. Huang, H., J. A. Ball, J. T. Billheimer, and F. Schroeder. 1999. Interaction of the N-terminus of sterol carrier protein-2 with membranes: role of membrane curvature. *Biochem. J.* **344**: 593–603.
 40. Kerkhoff, C., M. Beuck, J. Threige-Rasmussen, F. Spener, J. Knudsen, and G. Schmitz. 1997. Acyl-CoA binding protein (ACBP) regulates acyl-CoA:cholesterol acyltransferase (ACAT) in human mononuclear phagocytes. *Biochim. Biophys. Acta.* **1346**: 163–172.
 41. Rasmussen, J. T., N. J. Faergeman, K. Kristiansen, and J. Knudsen. 1994. Acyl-CoA-binding protein (ACBP) can mediate intermembrane acyl-CoA transport and donate acyl-CoA for beta-oxidation and glycerolipid synthesis. *Biochem. J.* **299**: 165–170.
 42. Herr, F. M., and D. E. Ong. 1992. Differential interaction of lecithin-retinol acyltransferase with cellular retinol binding proteins. *Biochemistry.* **31**: 6748–6755.
 43. Jamison, R. S., M. E. Newcomer, and D. E. Ong. 1994. Cellular retinoid-binding proteins: limited proteolysis reveals a conformational change upon ligand binding. *Biochemistry.* **33**: 2873–2879.
 44. Lee, R. G., M. C. Willingham, M. A. Davis, K. A. Skinner, and L. L. Rudel. 2000. Differential expression of ACAT1 and ACAT2 among cells within liver, intestine, kidney, and adrenal of nonhuman primates. *J. Lipid Res.* **41**: 1991–2001.
 45. Teasdale, R. D., and M. R. Jackson. 1996. Signal-mediated sorting of membrane proteins between the endoplasmic reticulum and the golgi apparatus. *Annu. Rev. Cell Dev. Biol.* **12**: 27–54.
 46. Chao, H., G. G. Martin, W. K. Russell, S. D. Waghela, D. H. Russell, F. Schroeder, and A. B. Kier. 2002. Membrane charge and curvature determine interaction with acyl CoA binding protein (ACBP) and fatty acyl CoA targeting. *Biochemistry.* **41**: 10549–10553.
 47. Davies, J. K., A. E. A. Thumser, and D. A. Wilton. 1999. Binding of recombinant rat liver fatty acid binding protein to small anionic phospholipid vesicles results in ligand release: a model for interfacial binding and fatty acid targeting. *Biochemistry.* **38**: 16932–16940.
 48. Petrescu, A. D., R. Hertz, J. Bar-Tana, F. Schroeder, and A. B. Kier. 2002. Ligand specificity and conformational dependence of the hepatic nuclear factor-4alpha (HNF-4a). *J. Biol. Chem.* **277**: 23988–23999.
 49. Butko, P., I. Hapala, G. Nemezc, and F. Schroeder. 1992. Sterol domains in phospholipid membranes: dehydroergosterol polarization measures molecular sterol transfer. *J. Biochem. Biophys. Meth.* **24**: 15–37.
 50. Hapala, I., J. Kavcansky, P. Butko, T. J. Scallen, C. Joiner, and F. Schroeder. 1994. Regulation of membrane cholesterol domains by sterol carrier protein-2. *Biochemistry.* **33**: 7682–7690.
 51. Rosendal, J., P. Ertbjerg, and J. Knudsen. 1993. Characterization of ligand binding to acyl-CoA-binding protein. *Biochem. J.* **290**: 321–326.
 52. Jolly, C. A., H. Chao, A. B. Kier, J. T. Billheimer, and F. Schroeder. 2000. Sterol carrier protein-2 suppresses microsomal acyl CoA hydrolysis. *Mol. Cell. Biochem.* **205**: 83–90.